ISSN (Online) 2456-1290

International Journal of Engineering Research in Mechanical and Civil Engineering (IJERMCE)

Vol 10, Issue 9, September 2023

Modeling Post-Infusion Application of Controlled External Pressure to a Polymer Composite Part

[1] Shevtsov S, [2]Zhilyaev I, [3]Chang S.-H, [4]Snezhina N, [5]Chai B.X

[1] South Center of Russian Academy of Science, [2] 9T Labs, Switzerland, [3] National Kaohsiung University of Science and Technology, Taiwan R.O.C., [4] Don State Technical University, Russia, [5] Swinburne University of Technology, Australia
[1] sergnshevtsov@gmail.com, [2] igor.zhilyaev@9tlabs.com, [3] shchang@nkust.edu.tw, [4] snezhina_nataly@mail.ru, [5] bchai@swin.edu.au

Abstract*— Vacuum infusion technologies are mainly used in the production of lightly loaded composite structures due to the relatively small and unevenly distributed of the fiber volume fraction and a significant variation in the wall thickness of finished parts, which is due to a significant internal pressure gradient in the preform upon completion of the infusion process. Some works have proposed and experimentally substantiated the application of controlled external pressure to the surface of the preform with a gradual increase in pressure in the vacuum vent and removal of excess resin. It has been established that the efficiency of the process depends on the duration, rate and maximum value of the applied pressure. This article presents a computer model of such a post-infusion process, supplementing the previously developed model of vacuum infusion, the simulation results of which are the initial conditions for the model presented below. The model is a finite element implementation of the coupled problem including Darcy's law, continuity and compressibility equations for a curable liquid resin and a compressed porous medium. The results of the process simulation give the distribution of pressure, porosity, wall thickness of the part during and after changes in controlled pressures, allowing you to achieve the best possible quality objectives for given resin and preform properties.

Index Terms*— Polymeric composite technology; post-infusion external pressure application; process modeling and optimization; vacuum infusion.

I. INTRODUCTION

The relatively low production costs, low volatile emissions associated with the process, and a possibility to produce composite parts with quite satisfactory strength characteristics for many applications make recent developments of vacuum-assisted resin transfer molding (VARTM) an attractive processing technique for the manufacture of large-scale composite structures [1]-[4]. However, each of them is characterized by the fact that the future composite product or part of it is a porous structure, the layers of which are unidirectional, oriented at different angles or fabrics, and liquid resin is introduced into such a porous body and propagates therein due to a pressure gradient generated. In general, all VARTM processes include three processing steps: material and tooling preparation, the filling of the liquid resin into the porous preform and the post-infusion step. Each step in the process determines key material quality factors, including strength properties, fiber volume fraction, void content and wall thickness variation. Unfortunately, some disadvantages inherent in these processes limit their use, especially in the manufacture of structures subjected to significant operational loads [4]-[6]. A detailed analysis justifiably indicates that the reasons for this drawback are the formation of the micro-voids and dry spots in the filled preform, the relatively low value of the fiber volume fraction and its uneven distribution in the body of the molded structure [7], [8]. For the subject of this article, these two properties of the infused preform are most important. The generally accepted fact that the preform is a compressible poroelastic frame, the pores of which are fully or partially filled with resin, makes obvious the relationship between the fiber volume fraction and the wall thickness of this preform. That is why, in the works devoted to the study of the fiber volume fraction, most often during the infusion process and after its completion, changes in the thickness of the preform are studied, as presented in articles [9]-[16]. The insufficient value of the fiber volume fraction V_f and, accordingly, increased porosity ϕ=1-V_f, their heterogeneous and complexly changing spatial distribution in the preform depend on the nature of the spreading resin front and, of course, on the geometry, permeability of the porous preform and the rheology of the resin, the viscosity of which is a function of time and temperature. This is the reason why, for many high-techs, e.g. aircraft applications VARTM does not currently provide sufficient repeatability or control of variability.

As a result of attempts to eliminate the listed shortcomings of the VARTM processes, a number of technical solutions have been developed. However, the most effective solution seems to be the technology of controlled post-infusion external pressure, proposed in [10], [11], various strategies of which [17]-[19] have received reliable experimental justification. Despite the fact that the proposed method requires some complication of technological equipment, it has the most realistic prospect of being introduced into the practice of manufacturing a wide range of polymer-composite structures. In the cited works of the

ISSN (Online) 2456-1290

International Journal of Engineering Research in Mechanical and Civil Engineering (IJERMCE)

Vol 10, Issue 9, September 2023

authors, studies were carried out with samples of preforms of relatively small sizes. Obviously, in order to obtain preliminary information about the parameters of the process when it is implemented on larger parts, it is necessary to understand how the size, shape of the parts and the use of other resins will affect the required process conditions. Such an understanding, which makes it possible to purposefully correct the sources of technological variability with the available means of control, can be achieved through the development of modeling tools and a detailed analysis of the results.

The history of the development of simulation tools for infusion processes dates back to the 90s of the last century. In most models [10], [14], [20]-[23], considerable attention is paid to the correct description of the compressive properties of porous preforms in both dry and wet states. For this, empirical compressibility models are used, most often of the power or polynomial type, and the compression pressure pc is taken in the simple form of the difference between the external pressure p_{ext} and the pore pressure p_m: $p_c = p_{ext} - p_m$. Due to the fact that verification of the validity of models for the evolution of the internal parameters of the system in the process is possible only with the use of an experimental assessment of the normal displacements of the surface of the molded preform and the applied pressure, deep meaningful works [11], [18], [19] developed dependences that couple local displacements of the preform surface with its strains, porosity and fiber volume fraction.

The present work is aimed at creating a tool for modeling the post-infusion stage of processes using dynamic pressure control described in [10], [11],]18], [19]. The authors of these papers rightly argue that the initial condition for the post-fill stage assumes that the form has been filled out completely. But this requirement cannot always be met, in particular, due to the presence of dry spots in the inner part or on the periphery of the preform. Such a situation often occurs in preforms of a complex shape - different-walled, with open "windows" or protruding elements [22]. Therefore, it is necessary to analyze the transitional stage of mold filling, and not just the steady state at the end of preform filling. Our project involves the integration of a previously developed software module for the infusion stage [22], [24] and the post-infusion stage simulation module described below. However, in the present version this module is stand-alone, using some reasonable assumptions about the initial distribution of pore pressure and porosity, which serve as initial conditions. When posing the problem of modeling the post-infusion stage, we tried to use the standings of poroelasticity as much as possible, especially in terms of describing the properties of an elastic porous frame, the influence of its dynamics on the flow of a viscous fluid, which satisfies the law of fluid mass continuity.

The text of the article is structured as follows. First of all, in order to clarify the information supplied by the input of the post-infusion stage simulation module, we briefly describe the composition of the results produced by the resin filling modeling module. Next, the used standings of poroelasticity are considered and their introduced simplifications for thin-walled porous volumes with transversal isotropy of the material are discussed. Further, with regard to the simplest geometry of a flat thin-walled rectangular plate, the relations used in the finite element (FE) implementation of the modeling problem are given. For one particular process control strategy, the time dependences of the compressive pressure applied to the outer surface of the preform and the pressure at the outlet are discussed. Some simulation results and their significance for application in the practice of manufacturing polymer composite structures are given in the final part of the article.

II. FE MODELING OF PREFORM RESIN FILLING

This modeling tool, described in our article [23], is designed to simulate the entire complex of phenomena in a preform of 3D geometry of arbitrary complexity, laid on an open mold, providing information about the ongoing process at each simulation time. Once the topological imperfections have been removed, the CAD model of the preform assembled with the open mold is imported into the Comsol Multiphysics environment, where the resin gate(s), vacuum vent(s), and High Permeability Medium (HPM) can be manually assigned (see Fig. 1). Thermal effect on all open surfaces is carried out by convective heat flux or infrared radiation [25].

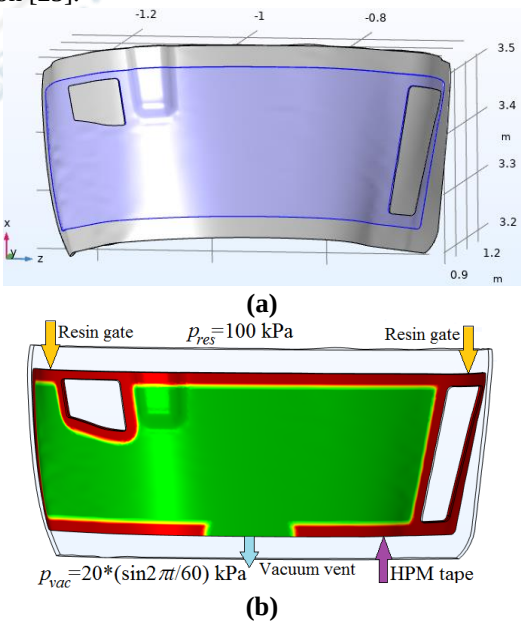

Figure 1. Geometry of modeled infused system: CAD model of the preform assembly with the mold (a); process layout - HPM tape, inlets and outlet location (b).

All phenomena are modeled by the coupled equations, including: the phase field equation describing the evolution of the interface between two moving phases - air and liquid

ISSN (Online) 2456-1290

International Journal of Engineering Research in Mechanical and Civil Engineering (IJERMCE)

Vol 10, Issue 9, September 2023

resin; the Richards equation, which reconstructs the pressure field p_m in a partially filled porous preform; a heat transfer equation and a kinetic/convection/diffusion equation for the resin's degree of cure α [22]. The coefficients of these equations are semi-empirical dependences of the fiber volume fraction V_f for the dry and wet preform on the compressive pressure p_c; the time and temperature dependences of degree of cure and resin viscosity μ_r. For the compressibility and thermal properties of a partially filled preform on saturation with liquid resin $V_r \in [0, 1]$, the mixing rule is used. Resin is initially injected into an empty preform at controlled pressure and temperature. The pressure in the vacuum line and the temperature on the exposed surfaces of the system are also controlled arbitrarily and independently. Changes in the most important parameters of the system (average, minimum and maximum values) over time (see Fig. 2) are recorded and visualized by means of post-processing. It is also possible to analyze the state of any parameter of the system at an arbitrary point in time (see Fig. 3).

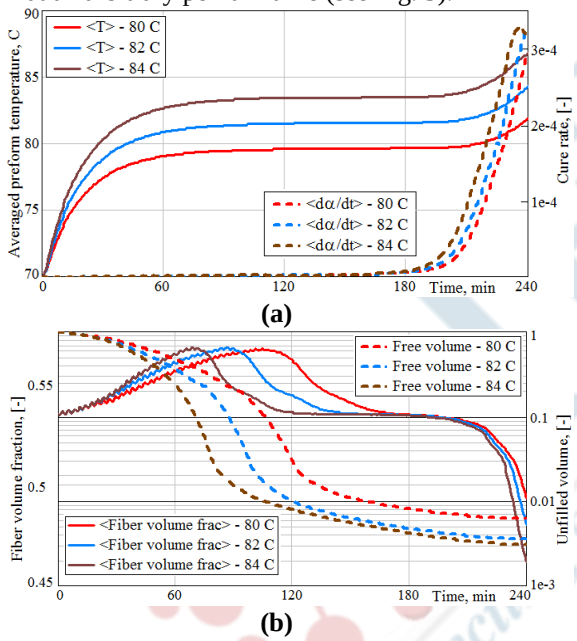

Figure 2. Plots of process parameters over time: (a) average temperature (°C) on exposed surfaces and cure rate; (b) relative preform void volume and average fiber volume fraction $<V_f>$.

If there are no dry spots in the infused preform, the simulation automatically stops when the minimum resin fill value of 0.9 is reached. Typically, at this point, the preform is 96-98% filled with resin. Figures 2, b and 3 demonstrate important features of the V_f evolution. At the initial infusion stage, when the area of the preform near the inlets is filled with resin, the preform volume contracts due to increasing its compressibility when wetted. At the final stage of the process, the pressure p_m in the preform increases and becomes more uniform, and the V_f decreases. The state of the preform at the end of the infusion step provides initial conditions for the operation of the post-infusion simulation module using dynamic pressure control. The formulation of the corresponding problem for one such post-infusion scenario and its FE implementation are given in the next section.

III. Modeling of Post-Infusion Stage

The approach presented below to a model statement is based on the concept of poroelasticity with simplifying assumptions due to the peculiarities of the shape of the infused preforms (relatively large thin-walled shell), their boundary conditions (the fixed fastening of their back surface to the forming mold) and transversal isotropy of the porous elastic frame.

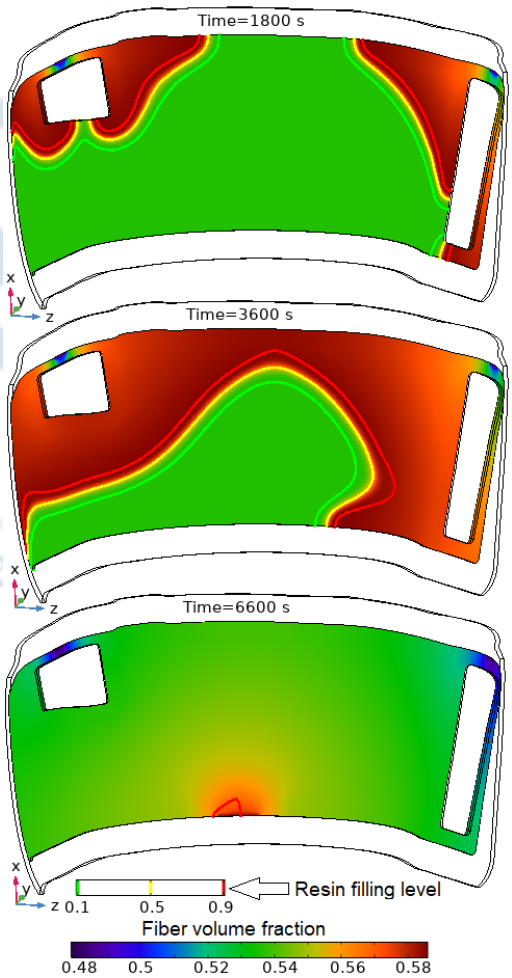

Figure 3. Spatial distribution of fiber volume fraction V_f and the location of the propagating resin front in the preform at three different times

Poroelasticity is used to describe the coupling between the solid and the interpenetrating fluid, where the solid is believed to be saturated by the fluid. It is an area of studying the movement/flow of material points in both the liquid phase and the solid skeleton. The modeling problem will be formulated in terms of the static poroelasticity, which accounts for a process in which fluid movement and solid skeleton deformation occur simultaneously and affect each

ISSN (Online) 2456-1290

International Journal of Engineering Research in Mechanical and Civil Engineering (IJERMCE)

Vol 10, Issue 9, September 2023

other. When statement the problem of the processes modeling, in the general case, the constitutive relations of poroelasticity [26] with the above listed simplifications are used as applied to an arbitrary preform geometry; however, these relations can be additionally simplified with a difference in the properties of the components - liquid, elastic frame, and reinforcing material (glass- or carbon fibers).

At the present stage of research, the purpose of which is to develop the post-infusion module and understand the processes occurring during its operation, it is decided most acceptable to conduct stand-alone simulations of this module. In this case, the initial conditions should be set by some relationships similar to those obtained as a result of the operation of the infusion module. In this regard, to ensure better convergence, the simplest preform geometry was adopted as a rectangular thin-walled flat plate. In addition, it is assumed that the preform is completely filled with liquid resin, and temperature, kinetic, and rheological changes are excluded from the model description.

A. Post-infusion modeling problem statement

A careful study of the methods of dynamic pressure control in the VARTM, presented in [18,] [19], shows that these methods are complicated versions of the classical Mandel problem [26], in which the process of outflow of a fluid contained in a porous body is studied under varying boundary conditions and applied pressures. The set of corresponding equations contains constitutive equations for the stress in poroelastic body and for internal pressure, the equilibrium equation, Darcy's law and continuity equation for the fluid content. By transformation, these equations are reduced to a system of three Navier-Cauchy equations for the displacement field **u** in a porous elastic body (which are not presented here because of their bulkiness), and to the diffusion equation for pore pressure p_m [26]

$$\partial p_m/\partial t - \kappa_x M\left(\partial^2 p_m/\partial x^2 + \partial^2 p_m/\partial y^2\right) - \kappa_z M\,\partial^2 p_m/\partial z^2 = \\ = -\alpha_x M\left(\partial e_{xx}/\partial t + \partial e_{yy}/\partial t\right) - \alpha_z M\,\partial e_{zz}/\partial t \quad (1)$$

The Navier-Cauchy equations contain the following elastic properties of a porous body with transversal isotropy: $M_{xx}, M_{xy}, M_{xz}, M_{zz}$ are the components of the stiffness matrix, which can be expressed through the Young moduli and Poisson ratio of the material; G and G' are the shear moduli in the *xy* and *xz* (*yz*) planes, respectively. The solution of the Navier-Cauchy system makes it possible to determine the volumetric strain from the relation $e = \nabla \cdot \mathbf{u}$ and its time derivatives

$$\left(\partial e_{xx}/\partial t; \partial e_{yy}/\partial t; \partial e_{zz}/\partial t\right) \quad (2)$$

which enters in (1). The so-called Biot modulus of the porous medium *M* is the reciprocal of the storage coefficient S_e measured under the condition of constant volume (constant deformation), which, neglecting the influence of the porous frame microstructure, is determined as [26]

$$S_e = 1/M = \phi/K_f + (1-\phi)/K_S - K/K_S^2, \quad (3)$$

where ϕ is a porosity, K_f is the bulk module of the fluid, K_s is the effective bulk modulus of the solid (reinforcement) phase, and K is the *drained* bulk modulus of the frame determined by the relationship

$$1/K = 1/K_S + \phi/K_\phi, \quad (4)$$

where K_ϕ is the pore volume bulk modulus. Equation (3) demonstrates a strong dependence of the K modulus on the elastic skeleton deformation, i.e. on actual porosity ϕ. The components of the Biot effective stress tensor $\boldsymbol{\alpha} = [\alpha_x; \alpha_x; \alpha_z; 0; 0; 0]$ in a case of transversely isotropic material are defined as [26]

$$\alpha_x = 1 - \left(M_{xx} + M_{xy} + M_{xz}\right)/3K_s \\ \alpha_z = 1 - \left(2M_{xz} + M_{zz}\right)/3K_s \quad (5)$$

The mobility tensor components $\boldsymbol{\kappa}$ in (1) are expressed in terms of the coefficients of the permeability tensor $\boldsymbol{k}$ and the dynamic viscosity of the resin μ_f as $\boldsymbol{\kappa} = \boldsymbol{k} / \mu_f$.

Our preliminary numerical experiments, in which the described post-infusion simulation module worked together with the infusion module (see Section II), taking its results as initial conditions, showed very slow convergence due to the high computational complexity of solving the Navier-Cauchy equations in local coordinate systems. To overcome this difficulty, a simplification was introduced, justified by the small thickness of the walls of the preform compared to its overall dimensions and the fixing of its inner surface on a stiff shaping mould. Neglecting the in-plane the preform deformations ($\varepsilon_x = \varepsilon_y = 0$), we assumed that it is compressible only in the out-of-plane direction. From this assumption follows the expression for the bulk modulus with constrained lateral boundaries of the elementary compressible volume

$$K_\phi = \tilde{Y}_z = Y_z/(1-2\nu_{zx})), \quad (6)$$

where Y_z is the Young module in the normal direction and *vzx* is the Poisson ratio. It should be additionally noted here that relation (4), which follows from the theory of poroelasticity, cannot be exactly fulfilled in systems like the one under consideration, since the porosity can never reach zero due to interlacing and microstructure of the system of reinforcing fibers. Therefore, the use of power-law or polynomial empirical models in most works to describe the dependence of the fiber volume fraction on compressive pressure can lead to gross errors at the significant compression of the preform. Assuming the use of increased compressive pressures in our study, we modified the function approximating the borrowed experimental results of [7] so that the fiber volume fraction does not exceed a certain limit value, taken equal to 0.62

$$V_f(p_c) = a \cdot \left[\tanh\left(\sqrt{p_c/p_1}\right) + \tanh\left(\sqrt{p_c/p_2}\right)\right] + c, \quad (7)$$

where coefficients a, c, p_1, p_2 founded by fitting

ISSN (Online) 2456-1290

International Journal of Engineering Research in Mechanical and Civil Engineering (IJERMCE)

Vol 10, Issue 9, September 2023

experimental data. In finite element models, a 3rd order splines approximation of this function, as well as the derivative of its inverse function, was used, which expresses the dependence of Y_z modulus on V_f (see Fig.4).

The accepted assumptions make it necessary to determine the effective compressive stress p_c, which depends on the applied external stress p_{appl} and pore pressure p_m according to

$$p_c = p_{appl} - \alpha_z \cdot p_m . \quad (8)$$

Further, using the dependence presented in Fig. 4,a, the values of the fiber volume fraction V_f, porosity ϕ, and the changed local thickness of the preform h are calculated as

$$\phi = 1 - V_f ; \quad h = h_0 \cdot (1-\phi_0)/(1-\phi), \quad (9)$$

where the indices "0" mean the initial values of the quantities.

The dependence in Fig. 4,b is used to determine the elastic modulus according to (6), and then calculate the volumetric strain rates (2) using (4), (5), (7) - (9). Thus, the introduced assumptions made it possible to abandon the solution of the Navier-Cauchy equations and close the algorithm for modeling the post-infusion stage of the process.

B. Standalone version of the post-infusion simulation FE module

The described model was formulated in Comsol Multiphysics FE software, in the Multiphysics mode. Due to the simplicity of the model geometry (see Fig. 5), all space variables were defined in the Global Coordinate System.

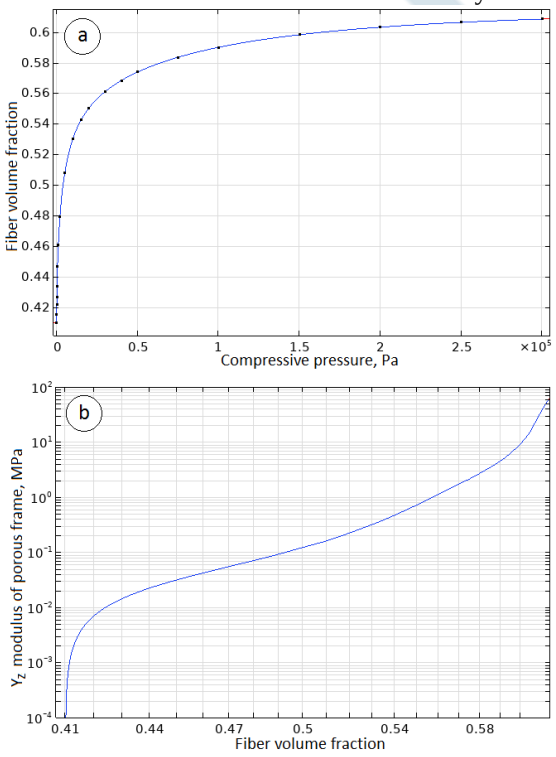

Figure 4. The semi-empirical dependencies of the fiber volume fraction V_f (a) and Young's modulus Y_z (b) on the compressive pressure for the wetted preform.

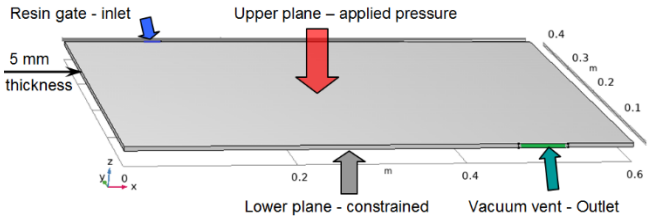

Figure 5. Geometry of the modeled system

The resin was fed into the preform through the inlet at atmospheric pressure p_{inl}=p_{atm}=100 kPa. The initial value of the pressure acting on the upper surface $p^0_{appl} = p_{atm}$ was also equal to atmospheric. The outlet pressure was initially p_{out}=20 kPa. The viscosity of the resin μ_f was taken unchanged throughout the simulation (see Fig. 6), and its spatial distribution was given by relation

$$\mu_f = 0.5 \cdot (0.1 + \tanh^2(d_{inl}/d_{max})) \text{ (Pa·s)}. \quad (10)$$

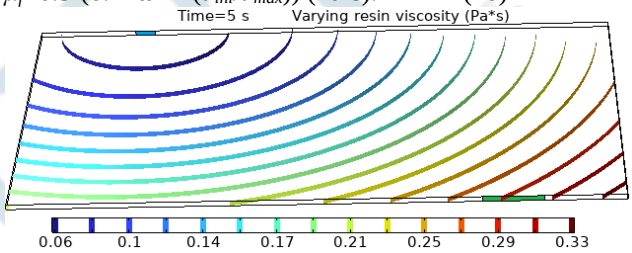

Figure 6. Resin viscosity distribution in the preform (not changing during simulation)

In this relation, d_{inl} is the distance from any point inside the preform to the inlet, and the maximum distance d_{max} was taken to be 0.64 m based on the geometry of the preform.

The simplifications presented above have reduced the problem to solving a single partial differential equation (PDE) of type (2). The described model was formulated using two Multiphysics nodes: Darcy's Law and Poroelasticity. Darcy's law in the non-stationary mode includes sub-nodes Porous medium, where the diffusion equation is presented in the form

$$\rho_f S_p \frac{\partial p_m}{\partial t} + \nabla \cdot \rho_f \left[-\boldsymbol{\kappa} (\nabla p_m) \right] = Q_m , \quad (11)$$

where for the Flow model the Darcy's flow is accepted, and Storage model S_p in the linearized form is a weighted sum of two compressibilities - of porous frame χ_p and of fluid χ_f, taken by the values $0.5 \cdot 10^{-9}$ Pa^{-1}

$$S_p = \phi \cdot \chi_f + (1-\phi)\, \chi_p . \quad (12)$$

The in-plane components of the permeability tensor are taken according to the Kozeny-Karman relation

$$K_x = K_y = K_{\min} \cdot \phi^3 / (1-\phi)^2 , \quad (13)$$

where $K_{\min}$ is taken for the investigated preform equal to $2 \cdot 10^{-11}$ m^2. Mass source Q_m in (11) is defined as

$$Q_m = -\rho_f \cdot \alpha_z \cdot de_z/dt . \quad (14)$$

In (14) ρ_f =1200 kg/m^3 is resin mass density, and for the time derivative of the volumetric strain, the value of the variable $e_z = (\phi - \phi_0)/(1-\phi)$ is differentiated with respect to

ISSN (Online) 2456-1290

International Journal of Engineering Research in Mechanical and Civil Engineering (IJERMCE)

Vol 10, Issue 9, September 2023

time by the built-in Comsol's operation. All preform boundaries are sealed (no flow condition), except for the inlet and outlet, where p_{inl} and p_{out} pressures are maintained.

The non-stationary problem for (11) is solved in two steps. The first step is to transform the initial pore pressure distribution in the preform to match it with Darcy's law. The function fitted by splines (see (Fig. 7)) corresponding to the results of numerical experiments obtained in [22], [24] was taken as the initial condition for $p_m^{in}(d_{inl}/d_{\max})$. The simulation of the post-infusion process began after the stabilization of the flow, when the mass flows of the fluid passing through the inlet and outlet became equal (see Fig. 8). During the first step no external conditions change. Two screenshots of the pore pressure for its initial distribution and one hour after the start of the simulation are shown in Fig.9.

At the second stage of modeling, the behavior of the system is studied under a controlled change in the boundary conditions. This article presents only one of the scenarios studied in the works [10], [18], [19] for the implementation of the post-infusion stage of the composite preform. Simulation of other scenarios requires changing the boundary conditions of the problem and choosing a different pressure control strategy. The scenario under consideration seems to be interesting and practically important in cases of fabrication of rather large-sized composite structures using highly active thermosetting resins, whose viscosity increases significantly during the process. This scenario is characterized by the fact that both the inlet and the outlet are open throughout the entire post-infusion stage, a constant atmospheric pressure is maintained at the inlet, and the laws of pressure control on the preform and at the outlet are regulated and depend on each other. In view of the importance of choosing the right strategy for managing these pressures, this issue will be considered first in the next section.

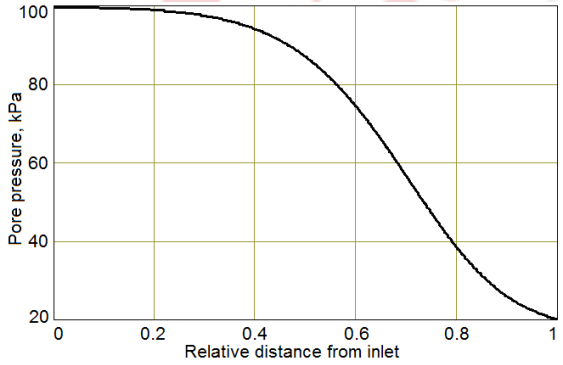

Figure 7. The dependence of the initial pore pressure p_m on the relative distance from inlet d_{inl}/d_{max}

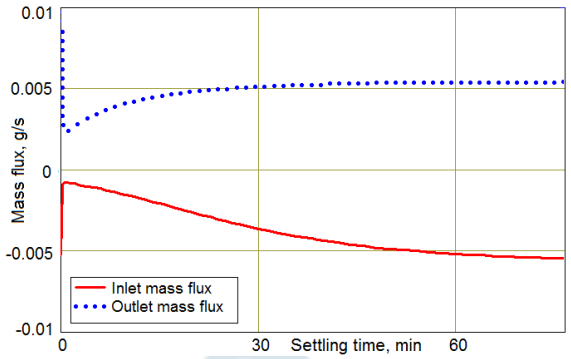

Figure 8. Preliminary stabilization of the resin flow

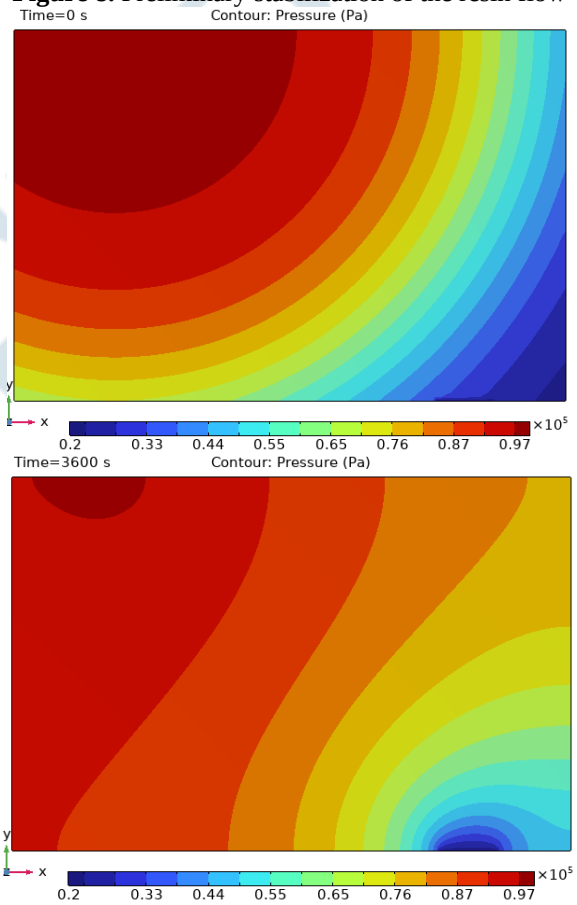

Figure 9. The initial pore pressure distribution and the result of its correction by the Darcy flow one hour later (Time=3600 s)

IV. CONSIDERATION AND ANALYSIS OF SIMULATION RESULTS

First of all, we note that for all the time dependences and screenshots presented below, the moment of the end of stabilization of the fluid flow process, i.e. the moment when the flows through the inlet and outlet became equal, is taken as the time reference point. For the case under consideration, the duration of the stage of settling the flow of resin is about 1 hr 20 min.

ISSN (Online) 2456-1290

International Journal of Engineering Research in Mechanical and Civil Engineering (IJERMCE)

Vol 10, Issue 9, September 2023

Before discussing the features of the system behavior at the next modeling step, we note the following. The sign of the flux depends on the orientation of the flow velocity vector relative to the normal vector to the boundary, which is always directed outward. Therefore, the flows of the fluid flowing from the inlet and outlet are positive, and vice versa, the inflows are negative. This is illustrated in Figure 10, which also shows the post-infusion control strategy. After start of the 2nd simulation step the flow of fluid flowing in through the inlet is negative, and the flow of fluid flowing out of the outlet is positive. Then there is a gradual increase in outlet pressure p_{out} from vacuum p_{vac}=20 kPa to atmospheric pressure p_{atm}. This increase in pressure must lag behind the increase in external pressure in time $\left(t_{start}^{out} > t_{start}^{pappl}\right)$, and the rate of these changes Δt^{out}, Δt^{appl} must take into account the inertia of the flow of liquid resin in the preform:

$$\begin{cases} p_{appl} = p_{atm} + p_{add}^{appl} \cdot H_2\left(t - t_{start}^{pappl}, \Delta t^{appl}\right) \\ p_{out} = p_{vac} + p_{add}^{out} \cdot H_2\left(t - t_{start}^{out}, \Delta t^{out}\right) \end{cases}, \quad (15)$$

where H_2 is the Heaviside function with a continuous 2nd derivative. The plots in Fig.10 show that the initially equal liquid resin fluxes abruptly change when subjected to controlled pressures, with the direction of resin flow in the inlet reversed from inward to outward. Further, the fluxes slowly change in magnitude, approaching zero.

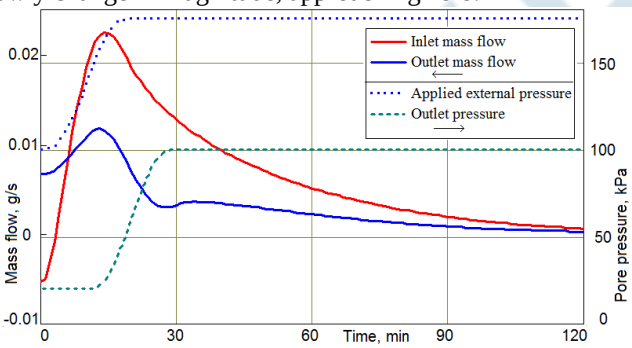

Figure 10. Mass fluxes of resin flowing from the inlet and outlet during preform compaction

Relationship (15) shows that the process control strategy depends on six parameters that can be changed: pressure increments $p_{add}^{appl}; p_{add}^{out}$, start time $t_{start}^{pappl}; t_{start}^{out}$ and duration $\Delta t^{appl}; \Delta t^{out}$ of their increase until a constant value is reached.

A rational choice of each of these controllable parameters should ensure the achievement of a minimum variation in porosity and preform wall thickness, eliminating the occurrence of critical situations. In particular, it is important to eliminate air from being drawn back into the preform through the bleed hole, and also to prevent return of previously displaced resin through the inlet. Only two out of many possible control scenarios are considered below. The boundary condition for the resin gate is different for these scenarios. In the first one, the inlet is open and the pressure in it is maintained equal to atmospheric $p_{inl}=p_{atm}$, due to which resin flushing occurs. In the second scenario, at the stage of resin flow stabilization, the inlet is open, but after stabilization is completed, the inlet closes immediately: **n**·**u**=0. Figures 11 - 13 show three groups of graphs for both scenarios, corresponding to a time lag $t_{start}^{pappl} = 0s; t_{start}^{out} = 20$ s; 30 s and to boost of vacuum vent pressure $p_{add}^{out} = 0$.

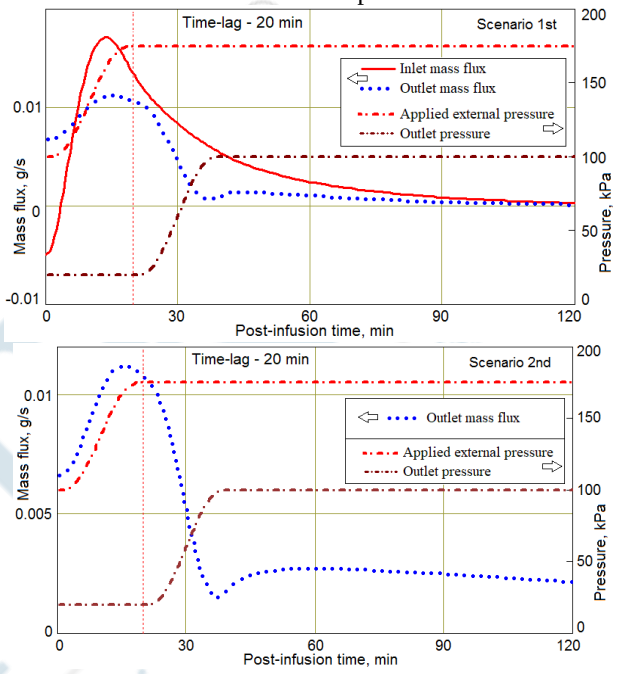

Figure 11. Time dependences of resin mass flows through the inlet and outlet for both scenarios at $t_{start}^{out} = 20s$

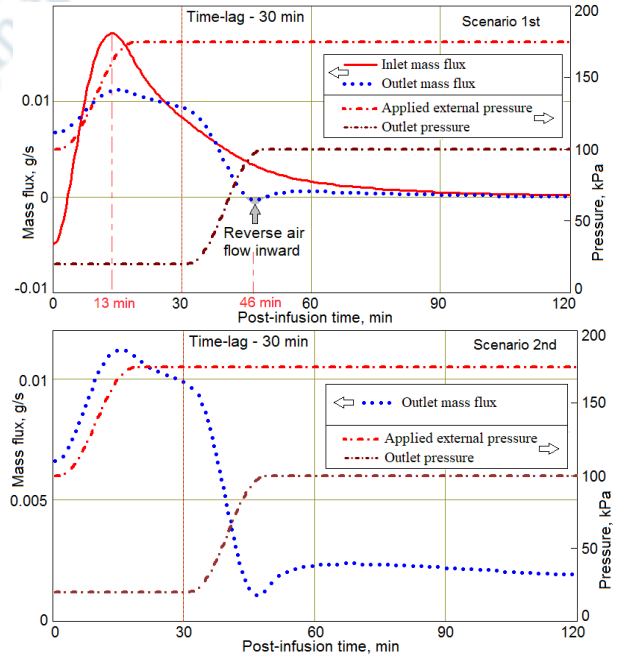

Figure 12. Time dependences of resin mass flows through the inlet and outlet for both scenarios at $t_{start}^{out} = 30s$

ISSN (Online) 2456-1290

International Journal of Engineering Research in Mechanical and Civil Engineering (IJERMCE)

Vol 10, Issue 9, September 2023

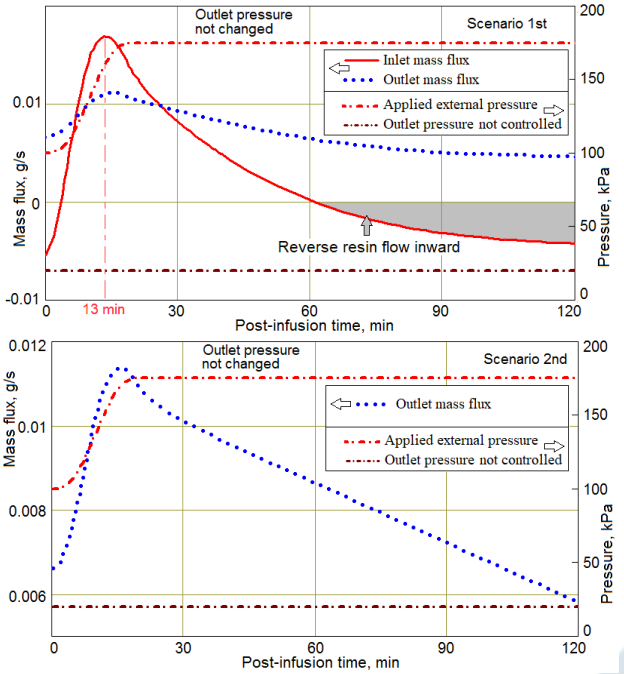

Figure 13. Time dependences of resin mass flows through the inlet and outlet for both scenarios at $p_{add}^{out} = 0$

Attention should be paid to two extremely undesirable situations presented in Fig. 12 for the 1st control scenario, which shows the reversal of the flow direction in the outlet. Namely, at the time of ~46 min this flux becomes directed inside the preform. But this means that the air contained in the resin trap will enter the preform. Fig. 13 shows the situation when the excess resin that came out of the inlet returns inward to the preform. Such phenomena must also be excluded, especially when using highly active thermosetting resins. These considered critical situations demonstrate the importance of choosing the right delay time and outlet pressure growth rate when using the first scenario. Note that when modeling the second scenario, no such situations were found. However, the simulation results, when varying the indicated modes of the post-infusion process according to the first scenario, make it possible to obtain the best indicators both in terms of quality (the maximum fiber volume fraction and the minimum of its dispersion, and wall thickness variations) with the minimum possible duration. As an example of the 1st scenario implementation, the Figs 14 and 15 show the time dependences of the average values and the spread of the porosity and wall thickness of the preform.

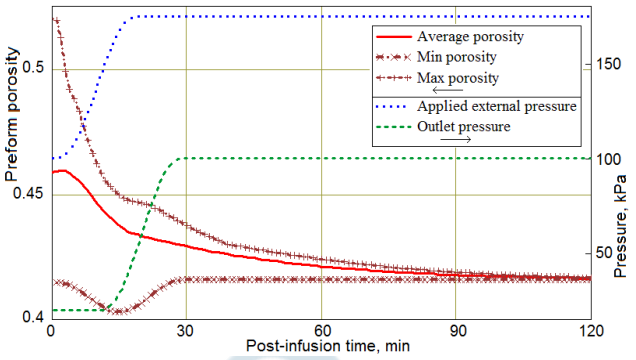

Figure 14. The evolution of the preform porosity superimposed with time dependences of controlled pressures

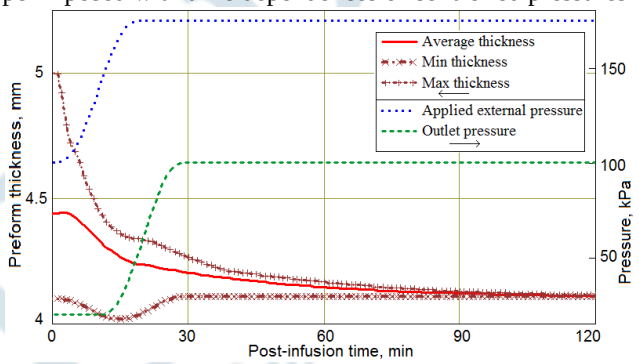

Figure 15. The evolution of the preform thickness superimposed with time dependences of controlled pressures

These plots demonstrate the efficient implementation of post-infusion controlled external pressure, which significantly improves the mean values and variance of preform porosity and wall thickness. However, it should be borne in mind that the actual post-infusion homogenization process may stop earlier due to the increase in viscosity of the thermosetting resin as a result of the increase in its degree of cure. Therefore, the autonomous simulation module presented in the paper is only a qualitative tool for understanding the dynamics of the process. Full quantitative process characterization can be achieved only with the joint operation of the infusion module [22], [24] and the modeling module presented above, which will allow taking into account temperature, thermokinetic effects that evolve over time. This ability is extremely important for the practice of manufacturing polymer-composite structures, since ever higher requirements are imposed on their geometric accuracy and stability, short-term and long-term strength, especially in the aircraft and rotorcraft industries.

REFERENCES

[1] A. Baker, S. Dutton and D. Kelly, Composite materials for aircraft structures. 2nd ed. (AIAA, Blacksburg, 2004) 600 p.

[2] D. Heider and J. W. Gillespie, "VARTM variability and substantiation," In The Joint Advanced Materials and Structures Center of Excellence (University of Delaware Center for Composite Materials), 12 p., 2008.

[3] K. K. Kar, Composite materials: processing, applications, characterizations. (Springer, Berlin Heidelberg, 2017) 690 p.

[4] O. A. Ekuase, N. Anjum, V. O. Eze and O. I. Okoli, "A Review on the Out-of-Autoclave Process for Composite Manufacturing," Journal of Composites Science, vol. 6, no.6, p. 172, June 2022.
[5] P. Celle, S. Drapier and J.-M. Bergheau, "Numerical modelling of liquid infusion into fibrous media undergoing compaction," European Journal of Mechanics A-Solid, vol. 27, no. 4, pp. 647-685, July 2008.
[6] M. J. Robinson and J. B. Kosmatka, "Analysis of the post-filling phase of the vacuum-assisted resin transfer molding process," Journal of Composite Materials, vol. 48, no. 13, pp. 1547-1559, May 2013.
[7] B. W. Grimsley, P. Hubert, X. L. Song, R. J. Cano, A. C. Loos, et al., "Flow and compaction during the vacuum assisted resin transfer molding process," NASA Technical Report, 15 p., Jan 2001.
[8] M. Y. Matveev, J. P-H. Belnoue, O. J. Nixon-Pearson, D. S. Ivanov, A. C. Long, et al., "A numerical study of variability in the manufacturing process of thick composite parts," Composite Structures, vol. 208, pp. 23-32, Jan 2019.
[9] S. M. R. Kazmi, Q. Govignon, and S. Bickerton., "Control of laminate quality for parts manufactured using the resin infusion process," Journal of Composite Materials, vol. 53, no. 3, pp. 327-343, June 2018.
[10] M. A. Yalcinkaya, E. M. Sozer, and M. C. Altan, "Effect of part thickness variation on the mold filling time in vacuum infusion process," Journal of Reinforced Plastics and Composites, vol. 33, no. 23, pp. 2136-2150, Dec 2014.
[11] C. Baris, B. Yenilmez, and E. Murat Sozer, "Modeling of post-filling stage in vacuum infusion using compaction characterization," Journal of Composite Materials, vol. 49, no. 16, pp. 1947-1960, July 2015.
[12] C. Arulappan, A. Duraisamy, D. Adhikari and S. Gururaja, "Investigations on pressure and thickness profiles in carbon fiber-reinforced polymers during vacuum assisted resin transfer molding," Journal of Reinforced Plastics and Composites, vol.34, no. 1, pp. 3-18, Jan 2015.
[13] T. Gajjar, D. B. Shah, S. J. Joshi and K. M. Patel, "Experimental study of thickness gradient and flow simulation in VARTM process," Fibers and Polymers, vol. 21, no. 2, pp. 384-391, Feb 2020.
[14] M. Mohamed, M. M. Selim, H. Ning and S. Pillay, "Effect of fiber prestressing on mechanical properties of glass fiber epoxy composites manufactured by vacuum-assisted resin transfer molding," Journal of Reinforced Plastics and Composites, vol.39, no. 1-2, pp. 21-30, Jan 2020.
[15] J. H. Shin, M. Anders, D. Kim, B. C. Jin, and S. Nutt, "Effects of post-infusion dwell on vacuum infusion of thermoset composites toughened by thermoplastic interlaminar veils," Journal of Composite Materials, vol. 55, no. 10, pp. 1419-1433, May 2021.
[16] D. Wu, R. Larsson and B. Blinzler, "A preform deformation and resin flow coupled model including the cure kinetics and chemo-rheology for the VARTM process," International Journal of Material Forming, vol. 14, no. 3, pp. 421-434, May 2021.
[17] D. U. Shah and M. J. Clifford, "Compaction, permeability and flow simulation for liquid Composite moulding of natural fibre composites," in Manufacturing of Natural Fibre Reinforced Polymer Composites (Springer, London), pp. 65-99, 2015.
[18] M. A. Yalcinkaya, E. M. Sozer, and M. C. Altan, "Fabrication of high quality composite laminates by pressurized and heated-VARTM," Composites Part A: Applied Science and Manufacturing, vol. 102, pp. 336-346, Nov 2017.
[19] M. A. Yalcinkaya, E. M. Sozer, and M. C. Altan, "Dynamic pressure control in VARTM: Rapid fabrication of laminates with high fiber volume fraction and improved dimensional uniformity," Polymer Composites, vol. 40, no. 6, pp. 2482-2494, June 2019.
[20] W. B. Young, "Three-dimensional modeling of the filling process in VARTM including the fiber compaction effect," International Journal of Advanced Engineering Technology, vol. 50, pp. 122-127, Mar 2016.
[21] F. Rubino and P. Carlone, "A Semi-Analytical Model to Predict Infusion Time and Reinforcement Thickness in VARTM and SCRIMP Processes," Polymers-Basel, vol. 11, no. 1, p. 20, Dec 2018.
[22] S. Shevtsov, I. Zhilyaev, S. H. Chang, J. K. Wu, N. Snezhina, et al., "Two-stage numerical approach for reliable recognition of dry spots at the VAP infusion of large composite parts of complex shape," Composite Structures, vol. 259, p.113437, Mar 2021.
[23] B. X. Chai, D. Eisenbart, M. Nikzad, B. Fox, A. Blythe, et al., "A novel heuristic optimisation framework for radial injection configuration for the resin transfer moulding process," Composites Part A: Applied Science and Manufacturing, vol. 165, p.107352, Feb 2023.
[24] S. Shevtsov, I. Zhilyaev, S. H. Chang, J. K. Wu, and N. Snezhina, "Multi-Criteria Decision Approach to Design a Vacuum Infusion Process Layout Providing the Polymeric Composite Part Quality," Polymers-Basel, vol. 14, no.2, p.313, Jan 2022.
[25] I. Zhilyaev,C. Brauner, S. Queloz, H. Jordi, R. Lüscher, et al., "Controlled curing of thermoset composite components using infrared radiation and mathematical modelling," Composite Structures, vol. 259, p. 113224, Mar 2021.
[26] A. H. D. Cheng, Poroelasticity. Theory and Applications of Transport in Porous Media (Springer International Publishing, Switzerland, 2016), 893 p.